14th Annual (International) Mechanical Engineering Conference – May 2006
Isfahan University of Technology, Isfahan, Iran

THEORETICAL ANALYSIS OF PIEZOELECTRIC HYBRID PLATES

M. Tahani [1], A.M. Naserian-Nik [2]
Department of Mechanical Engineering, Faculty of Engineering,
Ferdowsi University of Mashhad, Mashhad, Iran

mtahani@ferdowsi.um.ac.ir

Abstract
An analytical method is devlopteded to analyze piezoelectric hybrid laminated composite plates with arbitrary lamination and boundary conditions subjected to electromechanical loads. The method is based on separation of spatial variables of displacement field components. Within the displacement field of a first-order shear deformation plate theory and using the principle of minimum total potential energy, two systems of coupled ordinary differential equations with constant coefficients are obtained. These equations may be solved analytically with the help of state-space approach. Also a Levy-type solution is employed for verification the validity and accuracy of the proposed method. It is seen that the present results have close agreements with those obtained by Levy-type method.

Keywords: Analytical solution- Piezoelectric- Laminated plate- Boundary conditions.

Introduction
Hybrid composite plates consisting of fiber-reinforced and piezoelectric layers are important components of smart or intelligent structures ([1]-[3]). For the analytical solution of laminated composite plates, Pagano [4] firstly presented the exact solution of the laminated plate with simply supppted edges. Ray et al. [5,6] and Brooks and Heyliger [7] extended this methodology to develop a three-dimensional, exact, plane strain piezoelastic solution for simply supported single-layer and laminated piezoelectric plates with distributed and patched actuators. Three-dimensional, exact piezoelastic solutions for simply supported rectangular plates coupled to distributed sensors and actuators have been presented by Ray et al. [8], Heyliger [9,10] and Lee and Jiang [11]. Tauchert [12] applied the classical lamination theory (CLT) to obtain an analytical solution for a smart composite plate. Jonnalagadda et al. [13] employed first-order shear deformation theory (FSDT) to solve the piezothermoelastic response of hybrid plates with a known thermoelectric field. They presented a Navier-type solution for rectangular plates with all edges simply supported, and a finite element solution by using nine-noded Lagrangian elements, for plates with various edge support conditions. Huang and wu [14] have given a coupled, first-order shear deformation theory for the piezoelectric response of hybrid plates and a post-processing technique to obtain the accurate response of transverse stresses, transverse displacement, electric potential and electric displacement. A Levy-type solution for the bending of cross-ply, hybrid, rectangular plates with two opposite edges simply supported by using a mixed formulation of first-order shear deformation and classical lamination theories was presented by Kapuria et al. [15]. Senthil and Batra [16] provided the analytical solutions of piezoelectric laminated plates via Eshelby–Stroh formalism.

It can be seen most of avaiable analytical solution techniques for deformation of piezoelectric plates are restricted to whose edges are simply supported. Here, a new analytical method is developed to analyze laminated composite plates with arbitrary lamination and boundary conditions subjected to mechanical and electrical loads. Using the principle of minimum total potential energy and first-order shear deformation theory simultaneously, two

1-Assistant professor
2- M.S. student

systems of coupled ordinary differential equations with constant coefficients are obtained. The obtained equations are solved analytically using the state-space approach. In ordrer to verify the accuracy of the present theory a Levy-type solution for rectangular piezoelectric laminated plates with cross-ply and antisymmetric angle-ply laminations and two opposite edges simply supported using first-order shear deformation theory is employed. The comparison shows excellent agreement between the results.

Theory and formulation

Fig. 1 shows the geometric characteristics of hybrid multilayered plate considered herein, with side lengths *2a* and *2b* and total thickness *h*. The structure consists of arbitrary *N* orthotropic layers which some of them can be piezoelectric, with the spatial poling directions and a piezoelectric moduli such like exhibiting the crystal of class mm2.

Displacement and strain fields

Considering a rectangular cartesian coordinate system shown in Fig. 1, the displacement field components can be written as independent functions of the spatial variables using first-order shear deformation (FSDT) [17] theory as below:

$$\begin{aligned} u(x,y,z) &= u_i(x)\bar{u}_i(y) + z\psi_i(x)\bar{\psi}_i(y) \\ v(x,y,z) &= v_i(x)\bar{v}_i(y) + z\phi_i(x)\bar{\phi}_i(y) \\ w(x,y) &= w_i(x)\bar{w}_i(y) \end{aligned} \tag{1}$$

where $u(x,y,z)$, $v(x,y,z)$ and $w(x,y,z)$ are respectively the displacements in x, y and z directions, and $u_i(x)$, $\bar{u}_i(y)$, $v_i(x)$, $\bar{v}_i(y)$, $\psi_i(x)$, $\bar{\psi}_i(y)$, $\phi_i(x)$, $\bar{\phi}_i(y)$, $w_i(x)$, and $\bar{w}_i(y)$ are unknown functions. The infinitesimal strain tensor and the electric field vector are related to the mechanical displacement vector and the electric potential Φ by

$$\begin{aligned} &\varepsilon_x = \frac{\partial u}{\partial x}, \quad \varepsilon_y = \frac{\partial v}{\partial y}, \quad \varepsilon_z = \frac{\partial w}{\partial z} \\ &\gamma_{yz} = \frac{\partial v}{\partial z} + \frac{\partial w}{\partial y}, \\ &\gamma_{xz} = \frac{\partial u}{\partial z} + \frac{\partial w}{\partial y}, \quad \gamma_{xy} = \frac{\partial u}{\partial y} + \frac{\partial v}{\partial x} \end{aligned} \tag{2}$$

$$E_j = \Phi_{,j} \tag{3}$$

Substitution of the displacements (1) into Eqs. (2) strain-displacement relations yields.

$$\begin{aligned} \varepsilon_x &= u_i\bar{u}_i' + z\psi_i\bar{\psi}_i' = \varepsilon_x^0 + z\kappa_x \\ \varepsilon_y &= v_i\bar{v}_i' + z\phi_i\bar{\phi}_i' = \varepsilon_y^0 + z\kappa_y \\ \gamma_{yz} &= \phi_i\bar{\phi}_i + w_i\bar{w}_i' = \gamma_{yz}^0 \\ \gamma_{xz} &= \psi_i\bar{\psi}_i + w_i'\bar{w}_i = \gamma_{xz}^0 \\ \gamma_{xy} &= u_i\bar{u}_i' + v_i'\bar{v}_i + z(\psi_i\bar{\psi}_i' + \phi_i'\bar{\phi}_i) = \gamma_{xy}^0 + z\kappa_{xy} \\ \varepsilon_z &= 0 \end{aligned} \tag{4}$$

Equilibrium equations and boundary conditions

Now, using the principle of minimum total potential energy [18], two sets of equilibrium equations and boundary counditions corresponding to the independent variables can be shown to be:

$$\begin{aligned} &\delta u_i: \ \frac{dN_x^i}{dx} - N_{xy1}^i = 0, \\ &\delta v_i: \ \frac{dN_{xy2}^i}{dx} - N_y^i = 0 \\ &\delta \psi_i: \ \frac{dM_x^i}{dx} - M_{xy1}^i - Q_{x1}^i = 0 \\ &\delta \phi_i: \ \frac{dM_{xy2}^i}{dx} - M_y^i - Q_{y1}^i = 0 \\ &\delta w_i: \ \frac{dQ_{x2}^i}{dx} - Q_{y2}^i + q_i(x) = 0 \end{aligned} \tag{5}$$

and

$$\begin{aligned} &\delta \bar{u}_i: \ \frac{d\bar{N}_{xy1}^i}{dy} - \bar{N}_x^i = 0 \\ &\delta \bar{v}_i: \ \frac{d\bar{N}_y^i}{dy} - \bar{N}_{xy2}^i = 0 \\ &\delta \bar{\psi}_i: \ \frac{d\bar{M}_{xy1}^i}{dy} - \bar{M}_x^i - \bar{Q}_{x1}^i = 0 \\ &\delta \bar{\phi}_i: \ \frac{d\bar{M}_y^i}{dy} - \bar{M}_{xy2}^i - \bar{Q}_{y1}^i = 0 \\ &\delta \bar{w}_i: \ \frac{d\bar{Q}_{y2}^i}{dy} - \bar{Q}_{x2}^i + \bar{q}_i(y) = 0 \end{aligned} \tag{6}$$

where the generalized stress resultants, $q_i(x)$ and $\bar{q}_i(y)$ are defined as

$$\begin{aligned} \begin{bmatrix} \{N^i\}^T \\ \{M^i\}^T \\ \{\Theta^i\}^T \end{bmatrix} &= \begin{bmatrix} N_x^i & N_y^i & N_{xy1}^i & N_{xy2}^i \\ M_x^i & M_y^i & M_{xy1}^i & M_{xy2}^i \\ Q_{y1}^i & Q_{y2}^i & Q_{x1}^i & Q_{x2}^i \end{bmatrix} \\ &= \int_{-b}^{b} \begin{bmatrix} N_x\bar{u}_i & N_y\bar{v}_i' & N_{xy}\bar{u}_i' & N_{xy}\bar{v}_i \\ M_x\bar{\psi}_i & M_y\bar{\phi}_i' & M_{xy}\bar{\psi}_i' & M_{xy}\bar{\phi}_i \\ Q_y\bar{\phi}_i & Q_y\bar{w}_i' & Q_x\bar{\psi}_i & Q_x\bar{w}_i \end{bmatrix} dy \end{aligned} \tag{7}$$

$$\begin{aligned} \begin{bmatrix} \{\bar{N}^i\}^T \\ \{\bar{M}^i\}^T \\ \{\bar{\Theta}^i\}^T \end{bmatrix} &= \begin{bmatrix} \bar{N}_x^i & \bar{N}_y^i & \bar{N}_{xy1}^i & \bar{N}_{xy2}^i \\ \bar{M}_x^i & \bar{M}_y^i & \bar{M}_{xy1}^i & \bar{M}_{xy2}^i \\ \bar{Q}_{y1}^i & \bar{Q}_{y2}^i & \bar{Q}_{x1}^i & \bar{Q}_{x2}^i \end{bmatrix} \\ &= \int_{-a}^{a} \begin{bmatrix} N_xu_i' & N_yv_i & N_{xy}u_i & N_{xy}v_i' \\ M_x\psi_i' & M_y\phi_i & M_{xy}\psi_i & M_{xy}\phi_i' \\ Q_y\phi_i & Q_yw_i & Q_x\psi_i & Q_xw_i' \end{bmatrix} dx \end{aligned} \tag{8}$$

$$q_i(x) = \int_{-b}^{b} q(x,y)\,\bar{w}_i\,dy \tag{9}$$

$$\bar{q}_i(y) = \int_{-a}^{a} q(x,y)\,w_i\,dy \tag{10}$$

Also the stress resultants are

$$\begin{aligned} (N_x, N_y, N_{xy}, Q_y, Q_x) &= \int_{-h/2}^{h/2} (\sigma_x, \sigma_y, \sigma_{xy}, \sigma_{yz}, \sigma_{xz})dz \\ (M_x, M_y, M_{xy}) &= \int_{-h/2}^{h/2} (\sigma_x, \sigma_y, \sigma_{xy})z\,dz \end{aligned} \tag{11}$$

The boundary conditions consist of specifying the following quantities at the edges of the plate. For edges parallel to y-axis (i.e. $x=\pm a$):

Geometric (essential)		Force (natural)
u_i	or	N_x^i
v_i	or	N_{xy2}^i
ψ_i	or	M_x^i
ϕ_i	or	M_{xy2}^i
w_i	or	Q_{x2}^i

(12)

also, for edges parallel to x-axis (i.e. $y=\pm b$):

Geometric (essential)		Force (natural)
$\bar{u}_i$	or	$\bar{N}_{xy1}^i$
$\bar{v}_i$	or	$\bar{N}_y^i$
$\bar{\psi}_i$	or	$\bar{M}_{xy1}^i$
$\bar{\phi}_i$	or	$\bar{M}_y^i$
$\bar{w}_i(y)$	or	$\bar{Q}_{y2}^i$

(13)

Laminate constitutive relations

The linear constitutive relations for the kth orthotropic (piezoelectric) lamina in the laminate coordinates (x,y,z) are given in Eqs. (14). As a large electric potential difference is applied across one or more layers of the laminate, it is assumed that the electric field owing to the variation in stress (the direct piezoelectric effect) is insignificant compared with the applied electric field.

$$\sigma_{ij}^{(k)} = \bar{Q}_{ijmn}^{(k)} \varepsilon_{mn}^{(k)} - \bar{e}_{mij}^{(k)} E_m^{(k)} \tag{14}$$

In the above equations $\bar{Q}_{ijmn}^{(k)}$ denotes the transformed reduced plane-stress stiffness matrix and $\bar{e}_{mij}^{(k)}$ is the transformed piezoelectric moduli of the kth lamina. Upon substitution Eqs. (4) into Eqs. (14) and the subsequent results into Eqs. (11), the stress resultants are obtained which can be presented as follow:

$$\begin{Bmatrix} N_x \\ N_y \\ N_{xy} \\ M_x \\ M_y \\ M_{xy} \end{Bmatrix} = \begin{bmatrix} A_{11} & A_{12} & A_{16} & B_{11} & B_{12} & B_{16} \\ & A_{22} & A_{26} & B_{12} & B_{22} & B_{26} \\ & & A_{66} & B_{16} & B_{26} & B_{66} \\ & & & D_{11} & D_{12} & D_{16} \\ & sym. & & & D_{22} & D_{26} \\ & & & & & D_{66} \end{bmatrix} \begin{Bmatrix} \varepsilon_x^o \\ \varepsilon_y^o \\ \gamma_{xy}^o \\ \kappa_x \\ \kappa_y \\ \kappa_{xy} \end{Bmatrix} - \begin{Bmatrix} N_x^P \\ N_y^P \\ N_{xy}^P \\ M_x^P \\ M_y^P \\ M_{xy}^P \end{Bmatrix}$$

$$\begin{Bmatrix} Q_y \\ Q_x \end{Bmatrix} = k^2 \begin{bmatrix} A_{44} & A_{45} \\ A_{45} & A_{55} \end{bmatrix} \begin{Bmatrix} \gamma_{yz}^0 \\ \gamma_{xz}^0 \end{Bmatrix} - \begin{Bmatrix} Q_y^P \\ Q_x^P \end{Bmatrix} \tag{15}$$

Here k^2 (=5/6) is the shear correction factor of FSDT. Also A_{ij}, B_{ij}, and D_{ij} denote the extensional stiffnesses, the bending-extensional coupling stiffnesses, and the bending stiffnesses, respectively.

$$(A_{ij}, B_{ij}, D_{ij}) = \sum_{k=1}^{N} \int_{z_k}^{z_{k+1}} \bar{Q}_{ij}^{(k)} (1, z, z^2) dz \tag{16}$$

where N is the total number of layers. In Eqs. (15), $\{N^P\}$, $\{M^P\}$ and $\{Q^P\}$ are the electric stress resultants

$$\{N^P\}^T = \sum_{k=1}^{N_a} \int_{z_k}^{z_{k+1}} [\bar{e}_{31}^{(k)}, \bar{e}_{32}^{(k)}, \bar{e}_{36}^{(k)}] E_z^{(k)} dz$$

$$\{M^P\}^T = \sum_{k=1}^{N_a} \int_{z_k}^{z_{k+1}} [\bar{e}_{31}^{(k)}, \bar{e}_{32}^{(k)}, \bar{e}_{36}^{(k)}] E_z^{(k)} z\, dz \tag{17}$$

$$\{Q^P\} = \sum_{k=1}^{N_a} \int_{z_k}^{z_{k+1}} \begin{bmatrix} \bar{e}_{14} & \bar{e}_{24} & 0 \\ \bar{e}_{15} & \bar{e}_{25} & 0 \end{bmatrix}^{(k)} \{E\}^{(k)} dz$$

where N_a is the number of piezoelectric layers. Note that for layers other than piezoelectric layers, the parts containing piezoelectric moduli should be omitted.

Upon substitution of Eqs. (4) into (15) and the subsequent results into Eqs. (7) and (8) the generalized stress resultants are obtained which can be represented as follows:

$$\begin{Bmatrix} \{N^i\} \\ \{M^i\} \end{Bmatrix} = [A^{ij}] \{\xi_j\} - \begin{Bmatrix} \{N^{Pi}\} \\ \{M^{Pi}\} \end{Bmatrix}$$
$$\{\Theta^i\} = [B^{ij}] \{\eta_j\} - \{\Theta^{Pi}\} \tag{18}$$

$$\begin{Bmatrix} \{\bar{N}^i\} \\ \{\bar{M}^i\} \end{Bmatrix} = [\bar{A}^{ij}] \{\bar{\xi}_j\} - \begin{Bmatrix} \{\bar{N}^{Pi}\} \\ \{\bar{M}^{Pi}\} \end{Bmatrix}$$
$$\{\bar{\Theta}^i\} = [\bar{B}^{ij}] \{\bar{\eta}_j\} - \{\bar{\Theta}^{Pi}\} \tag{19}$$

where

$$\{\xi_j\} = [u_j' \quad v_j \quad u_j \quad v_j' \quad \psi_j' \quad \phi_j \quad \psi_j \quad \phi_j']^T$$
$$\{\eta_j\} = [\phi_j \quad w_j \quad \psi_j \quad w_j']^T \tag{20}$$

$$\{\bar{\xi}_j\} = [\bar{u}_j \quad \bar{v}_j' \quad \bar{u}_j' \quad \bar{v}_j \quad \bar{\psi}_j \quad \bar{\phi}_j' \quad \bar{\psi}_j' \quad \bar{\phi}_j]^T$$
$$\{\bar{\eta}_j\} = [\bar{\phi}_j \quad \bar{w}_j' \quad \bar{\psi}_j \quad \bar{w}_j]^T \tag{21}$$

and the generalized electric stress resultants and the stiffness coefficients A_{mn}^{ij}, B_{mn}^{ij}, $\bar{A}_{mn}^{ij}$ and, $\bar{B}_{mn}^{ij}$ are defined by

$$\begin{bmatrix} \{N^{Pi}\}^T \\ \{M^{Pi}\}^T \\ \{\Theta^{Pi}\}^T \end{bmatrix} = \int_{-b}^{b} \begin{bmatrix} N_x^P \bar{u}_i & N_y^P \bar{v}_i' & N_{xy}^P \bar{u}_i' & N_{xy}^P \bar{v}_i \\ M_x^P \bar{\psi}_i & M_y^P \bar{\phi}_i' & M_{xy}^P \bar{\psi}_i' & M_{xy}^P \bar{\phi}_i \\ Q_y^P \bar{\phi}_i & Q_y^P \bar{w}_i' & Q_x^P \bar{\psi}_i & Q_x^P \bar{w}_i \end{bmatrix} dy \tag{22}$$

$$\begin{bmatrix} \{\bar{N}^{Pi}\}^T \\ \{\bar{M}^{Pi}\}^T \\ \{\Theta^{Pi}\}^T \end{bmatrix} = \int_{-a}^{a} \begin{bmatrix} N_x^P u_i' & N_y^P v_i & N_{xy}^P u_i & N_{xy}^P v_i' \\ M_x^P \psi_i' & M_y^P \phi_i & M_{xy}^P \psi_i & M_{xy}^P \phi_i' \\ Q_y^P \phi_i & Q_y^P w_i & Q_x^P \psi_i & Q_x^P w_i' \end{bmatrix} dx \tag{23}$$

$$[A^{ij}] = \int_{-b}^{b} \left([\alpha] \otimes \{\xi_i\} \{\xi_j\}^T \right) dy$$
$$[B^{ij}] = \int_{-b}^{b} \left([\beta] \otimes \{\eta_i\} \{\eta_j\}^T \right) dy \tag{24}$$

$$\left[\overline{A}^{ij}\right]=\int_{-a}^{a}\left(\left[\alpha\right]\otimes\left\{\overline{\xi}_i\right\}\left\{\overline{\xi}_j\right\}^T\right)dx$$
$$\left[\overline{B}^{ij}\right]=\int_{-a}^{a}\left(\left[\beta\right]\otimes\left\{\overline{\eta}_i\right\}\left\{\overline{\eta}_j\right\}^T\right)dx \qquad (25)$$

where $[\alpha]$ and $[\beta]$ are

$$[\alpha]=\begin{bmatrix} A_{11} & A_{12} & A_{16} & A_{16} & B_{11} & B_{12} & B_{16} & B_{16} \\ & A_{22} & A_{26} & A_{26} & B_{12} & B_{22} & B_{26} & B_{26} \\ & & A_{66} & A_{66} & B_{16} & B_{26} & B_{66} & B_{66} \\ & & & A_{66} & B_{16} & B_{26} & B_{66} & B_{66} \\ & & & & D_{11} & D_{12} & D_{16} & D_{16} \\ & & sym. & & & D_{22} & D_{26} & D_{26} \\ & & & & & & D_{66} & D_{66} \\ & & & & & & & D_{66} \end{bmatrix} \qquad (26)$$

$$[\beta]=\begin{bmatrix} A_{44} & A_{44} & A_{45} & A_{45} \\ & A_{44} & A_{45} & A_{45} \\ & sym. & A_{55} & A_{55} \\ & & & A_{55} \end{bmatrix} \qquad (27)$$

It must be noted that the sign $\otimes$ used in Eqs. (24) and (25) is referred to *array multiplication* of two matrices.

Equilibrium equations in terms of displacements

The equilibrium equations (5) and (6) can be expressed in terms of displacements and electrical field by substituting the generalized stress resultants from (18) and (19). Hence, two sets of ordinary differential equations will be obtained as follows:

$$\begin{aligned}
&\delta u_i: A_{11}^{ij}u_j''+(A_{13}^{ij}-A_{31}^{ij})u_j'-A_{33}^{ij}u_j+A_{14}^{ij}v_j''+(A_{12}^{ij}-A_{34}^{ij})v_j'-A_{32}^{ij}v_j+A_{15}^{ij}\psi_j''+(A_{17}^{ij}-A_{35}^{ij})\psi_j'-A_{37}^{ij}\psi_j+A_{18}^{ij}\phi_j''\\
&\quad+(A_{16}^{ij}-A_{38}^{ij})\phi_j'-A_{36}^{ij}\phi_j=\frac{dN_x^{Pi}}{dx}-N_{xy1}^{Pi}\\
&\delta v_i: A_{41}^{ij}u_j''+(A_{43}^{ij}-A_{21}^{ij})u_j'-A_{23}^{ij}u_j+A_{44}^{ij}v_j''+(A_{42}^{ij}-A_{24}^{ij})v_j'-A_{22}^{ij}v_j+A_{45}^{ij}\psi_j''+(A_{47}^{ij}-A_{25}^{ij})\psi_j'-A_{27}^{ij}\psi_j\\
&\quad+A_{48}^{ij}\phi_j''+(A_{46}^{ij}-A_{28}^{ij})\phi_j'-A_{26}^{ij}\phi_j=\frac{dN_{xy2}^{Pi}}{dx}-N_y^{Pi}\\
&\delta\psi_i: A_{51}^{ij}u_j''+(A_{53}^{ij}-A_{71}^{ij})u_j'-A_{73}^{ij}u_j+A_{54}^{ij}v_j''+(A_{52}^{ij}-A_{74}^{ij})v_j'-A_{72}^{ij}v_j+A_{55}^{ij}\psi_j''+(A_{57}^{ij}-A_{75}^{ij})\psi_j'-(A_{77}^{ij}+B_{33}^{ij})\psi_j\\
&\quad+A_{58}^{ij}\phi_j''+(A_{56}^{ij}-A_{78}^{ij})\phi_j'-(A_{76}^{ij}+B_{31}^{ij})\phi_j-B_{34}^{ij}w_j'-B_{32}^{ij}w_j=\frac{dM_x^{Pi}}{dx}-M_{xy1}^{Pi}-Q_{x1}^{Pi}\\
&\delta\phi_i: A_{81}^{ij}u_j''+(A_{83}^{ij}-A_{61}^{ij})u_j'-A_{63}^{ij}u_j+A_{84}^{ij}v_j''+(A_{82}^{ij}-A_{64}^{ij})v_j'-A_{62}^{ij}v_j+A_{85}^{ij}\psi_j''+(A_{87}^{ij}-A_{65}^{ij})\psi_j'-(A_{67}^{ij}+B_{13}^{ij})\psi_j\\
&\quad+A_{88}^{ij}\phi_j''+(A_{86}^{ij}-A_{68}^{ij})\phi_j'-(A_{66}^{ij}+B_{11}^{ij})\phi_j-B_{14}^{ij}w_j'-B_{12}^{ij}w_j=\frac{dM_{xy2}^{Pi}}{dx}-N_y^{Pi}-Q_{y1}^{Pi}\\
&\delta w_i: B_{43}^{ij}\psi_j'-B_{23}^{ij}\psi_j+B_{41}^{ij}\phi_j'-B_{21}^{ij}\phi_j+B_{44}^{ij}w_j''+(B_{42}^{ij}-B_{24}^{ij})w_j'-B_{22}^{ij}w_j=\frac{dQ_{x2}^{Pi}}{dx}-Q_{y2}^{Pi}-q_i(x)
\end{aligned} \qquad (28)$$

$$\begin{aligned}
&\delta\overline{u}_i: \overline{A}_{33}^{ij}\overline{u}_j''+(\overline{A}_{31}^{ij}-\overline{A}_{13}^{ij})\overline{u}_j'-\overline{A}_{11}^{ij}\overline{u}_j+\overline{A}_{32}^{ij}\overline{v}_j''+(\overline{A}_{34}^{ij}-\overline{A}_{12}^{ij})\overline{v}_j'-\overline{A}_{14}^{ij}\overline{v}_j+\overline{A}_{37}^{ij}\overline{\psi}_j''+(\overline{A}_{35}^{ij}-\overline{A}_{17}^{ij})\overline{\psi}_j'-\overline{A}_{15}^{ij}\overline{\psi}_j+\overline{A}_{36}^{ij}\overline{\phi}_j''\\
&\quad+(\overline{A}_{38}^{ij}-\overline{A}_{16}^{ij})\overline{\phi}_j'-\overline{A}_{18}^{ij}\overline{\phi}_j=\frac{d\overline{N}_{xy1}^{Pi}}{dy}-\overline{N}_x^{Pi}\\
&\delta\overline{v}_i: \overline{A}_{23}^{ij}\overline{u}_j''+(\overline{A}_{21}^{ij}-\overline{A}_{43}^{ij})\overline{u}_j'-\overline{A}_{41}^{ij}\overline{u}_j+\overline{A}_{22}^{ij}\overline{v}_j''+(\overline{A}_{24}^{ij}-\overline{A}_{42}^{ij})\overline{v}_j'-\overline{A}_{44}^{ij}\overline{v}_j+\overline{A}_{27}^{ij}\overline{\psi}_j''+(\overline{A}_{25}^{ij}-\overline{A}_{47}^{ij})\overline{\psi}_j'-\overline{A}_{45}^{ij}\overline{\psi}_j+\overline{A}_{26}^{ij}\overline{\phi}_j''\\
&\quad+(\overline{A}_{28}^{ij}-\overline{A}_{46}^{ij})\overline{\phi}_j'-\overline{A}_{48}^{ij}\overline{\phi}_j=\frac{d\overline{N}_y^{Pi}}{dy}-\overline{N}_{xy2}^{Pi}\\
&\delta\overline{\psi}_i: \overline{A}_{73}^{ij}\overline{u}_j''+(\overline{A}_{71}^{ij}-\overline{A}_{53}^{ij})\overline{u}_j'-\overline{A}_{51}^{ij}\overline{u}_j+\overline{A}_{72}^{ij}\overline{v}_j''+(\overline{A}_{74}^{ij}-\overline{A}_{52}^{ij})\overline{v}_j'-\overline{A}_{54}^{ij}\overline{v}_j+\overline{A}_{77}^{ij}\overline{\psi}_j''+(\overline{A}_{75}^{ij}-\overline{A}_{57}^{ij})\overline{\psi}_j'-(\overline{A}_{55}^{ij}+\overline{B}_{33}^{ij})\overline{\psi}_j\\
&\quad+\overline{A}_{76}^{ij}\overline{\phi}_j''+(\overline{A}_{78}^{ij}-\overline{A}_{56}^{ij})\overline{\phi}_j'-(\overline{A}_{58}^{ij}+\overline{B}_{31}^{ij})\overline{\phi}_j-\overline{B}_{32}^{ij}\overline{w}_j'-\overline{B}_{34}^{ij}\overline{w}_j=\frac{d\overline{M}_{xy1}^{Pi}}{dy}-\overline{M}_x^{Pi}-\overline{Q}_{x1}^{Pi}\\
&\delta\overline{\phi}_i: \overline{A}_{63}^{ij}\overline{u}_j''+(\overline{A}_{61}^{ij}-\overline{A}_{83}^{ij})\overline{u}_j'-\overline{A}_{81}^{ij}\overline{u}_j+\overline{A}_{62}^{ij}\overline{v}_j''+(\overline{A}_{64}^{ij}-\overline{A}_{82}^{ij})\overline{v}_j'-\overline{A}_{84}^{ij}\overline{v}_j+\overline{A}_{67}^{ij}\overline{\psi}_j''+(\overline{A}_{65}^{ij}-\overline{A}_{87}^{ij})\overline{\psi}_j'-(\overline{A}_{85}^{ij}+\overline{B}_{13}^{ij})\overline{\psi}_j\\
&\quad+\overline{A}_{66}^{ij}\overline{\phi}_j''+(\overline{A}_{68}^{ij}-\overline{A}_{86}^{ij})\overline{\phi}_j'-(\overline{A}_{88}^{ij}+\overline{B}_{11}^{ij})\overline{\phi}_j-\overline{B}_{12}^{ij}\overline{w}_j'-\overline{B}_{14}^{ij}\overline{w}_j=\frac{d\overline{M}_y^{Pi}}{dy}-\overline{M}_{xy2}^{Pi}-\overline{Q}_{y1}^{Pi}\\
&\delta\overline{w}_i: \overline{B}_{23}^{ij}\overline{\psi}_j'-\overline{B}_{43}^{ij}\overline{\psi}_j+\overline{B}_{21}^{ij}\overline{\phi}_j'-\overline{B}_{41}^{ij}\overline{\phi}_j+\overline{B}_{22}^{ij}\overline{w}''+(\overline{B}_{24}^{ij}-\overline{B}_{42}^{ij})\overline{w}_j'-\overline{B}_{44}^{ij}\overline{w}_j=\frac{d\overline{Q}_{y2}^{Pi}}{dy}-\overline{Q}_{x2}^{Pi}-\overline{q}_i(y)
\end{aligned} \qquad (29)$$

Solution of equations

Here, we employed the state-space approach [19] to solve the equilibrium equations obtained in the previous section. The linear system of ordinary differential equations (28) can be expressed in the form of single, first-order, matrix differential equation

$$\{X'\}=[C]\{X\}+\{F\} \qquad (30)$$

where the state vector $\{X\}$ is defined as

$$\{X_1\}=\{u_j'\},\ \{X_2\}=\{v_j\},\ \{X_3\}=\{u_j\},\ \{X_4\}=\{v_j'\},$$
$$\{X_5\}=\{\psi_j'\},\ \{X_6\}=\{\phi_j\},\ \{X_7\}=\{\psi_j\},$$
$$\{X_8\}=\{\phi_j'\},\ \{X_9\}=\{w_j'\},\ \{X_{10}\}=\{w_j\} \quad (31)$$

In order to solve Eq. (30) a solution is assumed which satisfies the associated boundary conditions at $y=\pm b$. In other words, by assuming solutions for $\bar{u}_i(y), \bar{u}_i'(y), \ldots, \bar{w}_i'(y)$ the components of matrix [C] and vector {F} can be easily calculated. The general soluion of Eq. (30) is given by [20]:

$$\{X\}=[U][Q]\{K\}+[U][Q]\int_x [Q]^{-1}[U]^{-1}\{F\}dx \quad (32)$$

where [U] is the matrix of distinct eigenvectors of matrix [C] and {K} is a vector of unknown constants to be found by imposing the boundary conditions at edges $x=\pm a$. Also the diagonal matrix [Q] is defined as

$$[Q]=diag(e^{\lambda_1 x}, e^{\lambda_2 x}, \ldots, e^{\lambda_{10} x}) \quad (33)$$

where λ_k $(k=1,2,\ldots,10)$ are the eigenvalues associated with matrix [C].

Using the solutions obtained from the system of equations (28) the system of differential equations (29) can be solved similarly. This procedure (solving the coupled systems of ordinary differential equations) will be continued until the solutions of the two systems are converged.

Numerical results and discussion

In accordance with the theoretical methodology developed in the previous sections, two problems involving various sets of boundary conditions are examined. The hybrid rectangular plates studied in these problems are made up of graphite/epoxy laminae of equal thickness and piezoelectric layers of polyvinylidene fluoride (PVDF). The material constants of PVDF [21] and the graphite/epoxy laminae [13] are listed in Table 1.

As a benchmark, a Levy-type solution based on FSDT is developed. It is well known that a Levy 's solution exists only for cross-ply and antisymmetric angle-ply laminates with two opposite edges simply supported. In example 1 results obtained utilizing the present method are compared with those obtained by the Levy-type solution for a general cross-ply hybrid laminate with admissible boundary conditions. Also in example 2 a hybrid laminate with other lamination and boundary conditions that there exist no Levy-type solutions will be studied.

Denoting simply supported, clamped and free boundary conditions by S, C and F, a 4-word notation such as SFSC is employed to show the boundary conditions on the four edges of the plate. The 1-4th word indicates the boundary conditions on edges $x=-a$, $y=-b$, $x=a$ and $y=b$ respectively. Two types of simple supports are applied at the edge of the laminate, which is classified as:

S1:

$$v_i=w_i=\phi_i=N_x^i=M_x^i=0 \quad \text{at } x=\pm a \quad (34a)$$

$$u_i=w_i=\psi_i=N_y^i=M_y^i=0 \quad \text{at } y=\pm b \quad (34b)$$

S2:

$$u_i=w_i=\phi_i=N_{xy}^i=M_x^i=0 \quad \text{at } x=\pm a \quad (35a)$$

$$v_i=w_i=\psi_i=N_{xy}^i=M_y^i=0 \quad \text{at } y=\pm b \quad (35b)$$

It is to be noted that S1 is used for cross-ply laminates and S2 is used for antisymmetric angle-ply laminates to obtain Levy's solutions.

Example 1:

First a numerical example is presented for hybrid rectangular plate [p/0°/90°/90°/0°], which p denotes piezoelectric layer. The plate has length-to-width ratio a/b=2 and width-to-thickness ratio 2b/h=10. The upper surface of double-thickness piezopolymer is subjected to a uniform electric potential $\Phi=\Phi_0$ or a sinusoidal potential $\Phi=\Phi_0\cos\frac{\pi x}{2a}\cos\frac{\pi y}{2b}$ and its lower surface is grounded ($\Phi=0$). In addition, it is assumed that the variation of electric potential is linear through the piezoelectric layer. In the case of applied uniform potential, the results achived from the present method and the Levy method are compared by Figs. 2-4. All the numerical results for deflections and stresses shown in what follows are nondimensionalized as below:

$$\bar{w}=w\left(\frac{-E_p}{e_{32}\Phi_0}\right)$$
$$(\bar{\sigma}_x,\bar{\sigma}_y,\bar{\sigma}_{xy})=(\sigma_x,\sigma_y,\sigma_{xy})\left(\frac{2b}{e_{32}\Phi_0}\right)\times 10^{-1} \quad (36)$$
$$(\bar{\sigma}_{xz},\bar{\sigma}_{xz})=(\sigma_{xz},\sigma_{xz})\left(\frac{2b}{e_{32}\Phi_0}\right)$$

where E_p denotes the Young's moduli of PVDF layer. The variation of nondimensionalized deflection versus $x/2a$ at $y=0$ is shown in Fig. 2 corresponding to three sets of CSCS, FSFS and FSCS boundary counditions. Also Figs. 3 and 4 illustrate the distributions of normal stress $\bar{\sigma}_y(0,0,z/h)$ and transvers shear stress $\bar{\sigma}_{xz}(a/2,b/2,z/h)$ through the thickness of described hybrid plate under various boundary conditions. It is to be noted that the numerical values of interlaminar stresses are obtained by integrating the local equilibrium equations of elasticity.

It is seen in the above mentioned figures that there are close agreements between the present results and those obtained by Levy 's solution. However, it can be seen that the magnitude of errors are different depending on the type of boundary conditions imposed on the edges of the plate.

The through-thickness variations of shear stresses $\bar{\sigma}_{xy}(a,b,z/h)$ and $\bar{\sigma}_{xz}(a/2,b/2,z/h)$ due to the applied

sinusoidal potential are shown in Figs. 5 and 6 respectively. In this case there is no difference between Levy 's solutions.

Example 2:

To demonstrate the applicability of the proposed method to analyze hybrid laminated plates with arbitrary lamination and boundary conditions, as the second example square hybrid plate [*p*/45°/90°/-45°/*p*] with the aspect ratio 10 is considered.

Two piezocelectric layers bonded to the top and bottom surfaces of the laminate have equal thicknesses of h/10. A sinusoidal potential of peak amplitude of Φ_0 is applied to the upper and lower surfaces of the plate, with the other surfaces of piezoelectric layers grounded.

The variation of deflection at y=0, along the length of the plate with four sets of boundary conditions: SSSS, CCCC, CFCF and CFSF, is presented in Fig. 7. As expected, the curves corresponding to boundary conditions CCCC and SSSS are located above and below the other curves respectively.

Figs 8 and 9 depicts the through-thickness distributions of normal stress $\bar{\sigma}_y(0,0,z/h)$ and transvers shear stress $\bar{\sigma}_{yz}(a/2,b/2,z/h)$ for different sets of boundary conditions.

Conclusion

A new analytical method is developed to study the bending behavior of hybrid piezoelectric laminates. In spite the procedure is simple, the proposed method has the capability for analyzing hybrid plates with arbitrary lamination and boundary conditions.

Using the Levy-type solution as a benchmark, the excellent agreement beween the present results for several sets of boundary conditions, especially in the case of applied sinusoidal potential, are found. Generally, for the case in which the plate is subjected to a uniform electric potential the amount of generated error depends on the type of boundary conditions imposed on the edges of the plate.

It is expected that increasing the number of terms in the assumed displcement field, may improves the accuracy of the results obtained by the proposed method.

References

[1] R.G. Loewy, Recent developments in smart structures with aeronautical applications, Smart Mat. Struct. 6 1997, R11-R42.

[2] E. Crawley, J. de Luis, Use of piezoelectric actuators as element of intelligent structures, AIAA J. 25(10) 1987, 1373-85.

[3] C.K. Lee, F.C. Moon. Laminated piezopolymer plates for torsion and bending sensors and actuators, J. Acoust. Soc. Am. 85(6) 1989, 2432-39.

[4] N.J. Pagano, Exact Solutions for Rectangular Bidirectional Composites and Sandwich Plates, Journal of Composite Materials 4 1970, 20-34.

[5] M.C. Ray, K.M. Rao, B. Samanta, Exact analysis of coupled electroelastic behaviour of a piezoelectric plate under cylindrical bending, Comput Struct 1992 45(4), 667–77.

[6] M.C. Ray, K.M. Rao, B. Samanta, Exact solution for static analysis of an intelligent structure under cylindrical bending, Comput Struct 1993 47(6),1031–42.

[7] Brooks, S. and Heyliger, P., Static behavior of piezoelectric laminates with distributed and patched actuators, J. Intelligent Mater. Systems Struc 1994 5, 635-646.

[8] M.C. Ray, R. Bhattacharya, B. Samanta, Exact solutions for static analysis of intelligent structures, AIAA J. 1993 31(9),1684–91.

[9] P. Heyliger, Static behavior of laminated elastic/ piezoelectric plates, AIAA J., 1994 32, 2481-84.

[10] P. Heyliger, S. Brooks, Exact solutions for laminated piezoelectric plates in cylindrical bending, J. Appl. Mech. 1996 63(4), 903–10.

[11] J.S. Lee, L.Z. Jiang, Exact electroelastic analysis of piezoelectric laminate via state space approach, Int. J. Solids Struct, 1996 33, 977-90.

[12] T.R. Tauchert, Piezothemoelastic behavior of a laminate, J. Thermal Stresses, 1992 15, 25-37.

[13] K.D. Jonnalagadda, G.E. Blandford, T.R. Tauchert, Piezothermoelastic composite plate analysis using first-order shear deformation theory, Comput. Struct 1994, 51, 79-89.

[14] J.H. Huang, T.N. Wu, Analysis of hybrid multilayered piezoelectric plates, Int. J. Eng. Sci. 1996, 34, 171-181.

[15] S. Kapuria, G.P. Dube, P.C. Dumir and S. Sengupta, Levy-type piezothermoelastic solution for hybrid plate by using first-order shear deformation theory, *Composites Part* B 28B 1997, 535-46.

[16] S. Senthil, R.C. Batra, Cylindrical bending of laminated plates with distributed and segmented piezoelectric actuators/sensors, AIAA J. 2000 38(5), 857–67.

[17] J.N. Reddy, Mechanics of laminated composite plates and shells, CRC Press, 2nd edition., 2004.

[18] Fung, Y.C., Foundation of solid Mechanics, Prentice-Hall, Englewood Cliffs, New Jersey, 1st edition, 1965.

[19] J.L. Goldberg, A.J. Schwartz, Systems of ordinary differential equations, An Introduction, Harper and Row, New York, 1972.

[20] J.N. Franklin, Matrix theory, Prentice-Hall, Englewood Cliffs, New Jersey, 1968.

[21] J.F. (Ed.) Shackelford, Materials science and engineering handbook, 2th edition, CRC Press, London, 1994, pp. S190.

Table 1. Material properties of graphite/epoxy and PVDF

Property	graphite/epoxy	PVDF
E_1 (GPa)	181	2.0
E_2	10.3	2.0
G_{12}	7.17	0.752
G_{23}	2.87	0.752
G_{31}	7.17	0.752
υ_{12}	0.28	0.33
e_{31} (Cm^{-2})	-	0.0687
e_{32}	-	0.0687

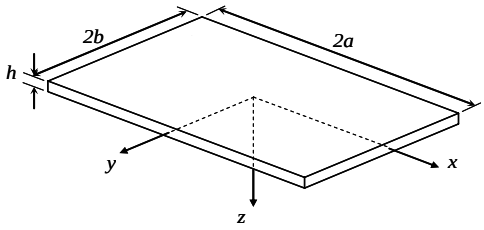

Fig. 1. The plate geometry and coordinate system.

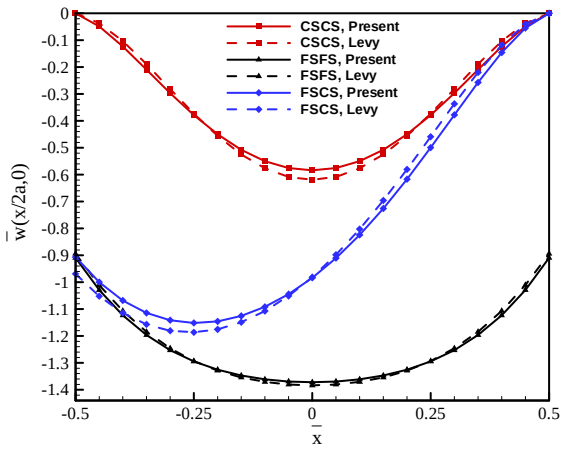

Fig. 2. Variations of deflection versus *x/2a* for a hybrid plate [*p*/0°/90°/90°/0°] subjected to the uniform potential.

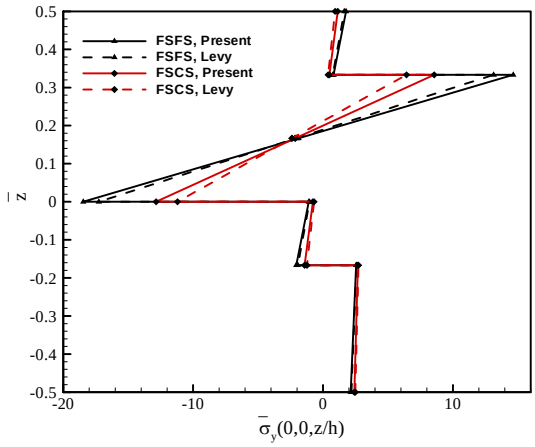

Fig. 3. Variations of normal stress $\bar{\sigma}_y(0,0,z/h)$ through the thickness of a hybrid plate [*p*/0°/90° /90°/0°] subjected to the uniform potential.

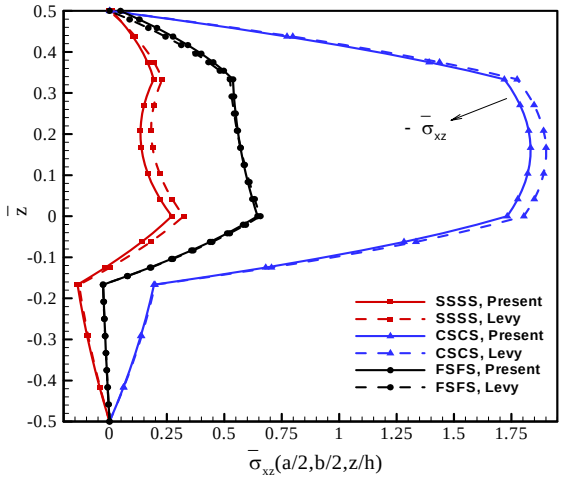

Fig. 4. Distributions of transvers shear stress $\bar{\sigma}_{xz}(a/2,b/2,z/h)$ through the thickness of a hybrid plate [*p*/0°/90°/90°/0°] subjected to the uniform potential.

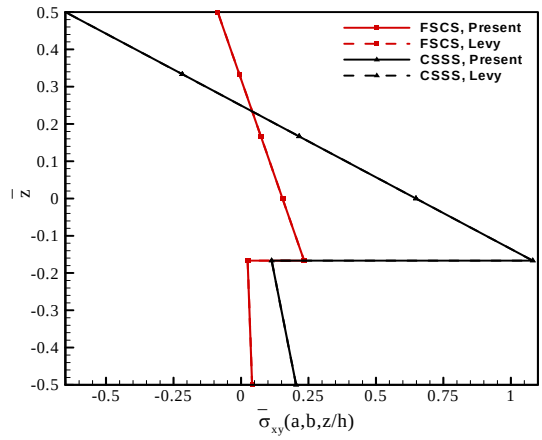

Fig. 5. Variations of shear stress $\bar{\sigma}_{xy}(a,b,z/h)$ through the thickness of a hybrid plate [p/0°/90°/90°/0°] subjected to the sinusoidal potential.

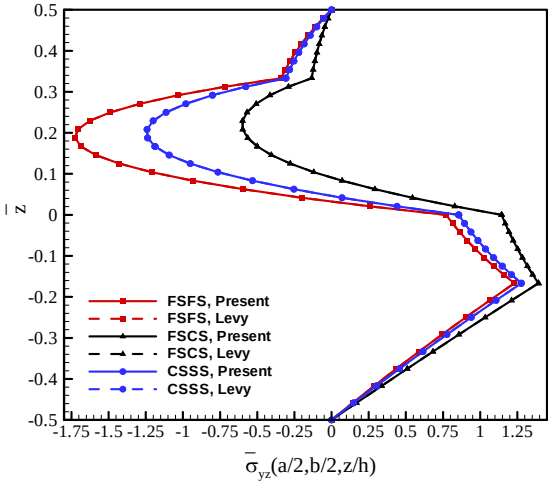

Fig. 6. Distributions of transvers shear stress $\bar{\sigma}_{yz}(a/2,b/2,z/h)$ through the thickness of a hybrid plate [p/0°/90°/90°/0°] subjected to the sinusoidal potential.

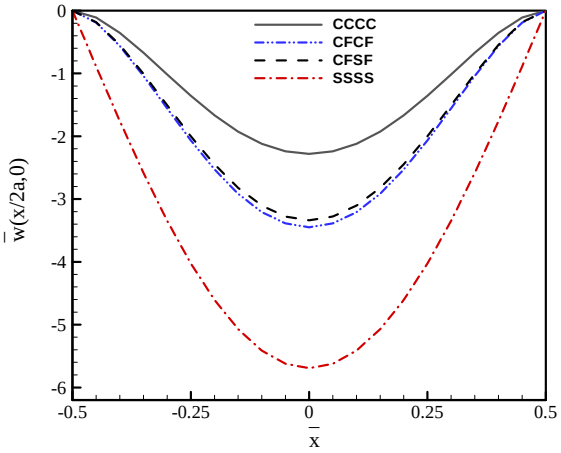

Fig. 7. Variations of deflection versus $x/2a$ at y=0 for a hybrid plate [p/45°/90°/-45°/p] subjected to the sinusoidal potential.

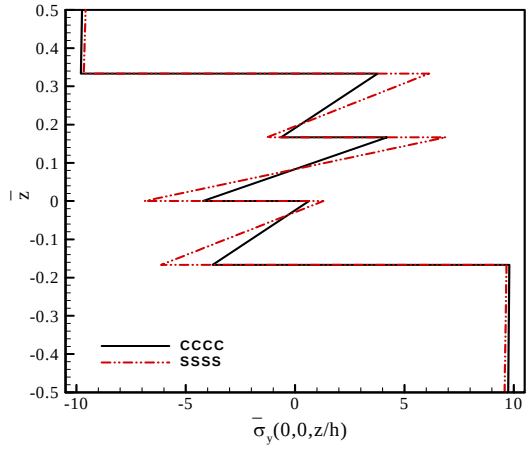

Fig. 8. Variations of normal stress $\bar{\sigma}_{y}(0,0,z/h)$ through the thickness of a hybrid plate [p/45°/90° /-45°/p] subjected to the sinusoidal potential.

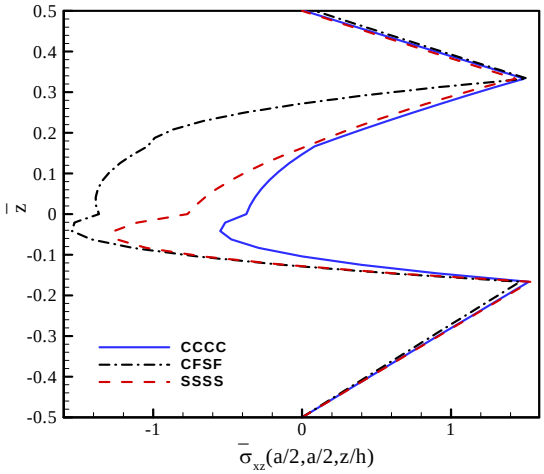

Fig. 9. Distributions of transvers shear stress $\bar{\sigma}_{xz}(a/2,b/2,z/h)$ through the thickness of a hybrid plate [p/45°/90°/-45°/p] subjected to the sinusoidal potential.